Electronic Supplementary Material (ESI) for Journal of Materials Chemistry C.


# Laser Annealing of Electrodeposited $CuInSe_2$ Semiconductor Precursors: Experiment and Modeling

H. J. Meadows, S. Misra, B. J. Simonds, M. Kurihara, T. Schuler, V. Reis-Adonis, A. Bhatia, M. A. Scarpulla, and P. J. Dale

**Supplementary information**

**Calculation of composition and free energy of coelectrodeposited precursor**

The free energy of the as co-electrodeposited precursor was estimated from depth profiled elemental composition data. Figure SI1 shows that the elements are not uniform through the depth evidencing that as well as the ternary $CuInSe_2$, other binary and elemental phases must also be present.

The principle behind the calculation was as follows:

1) The depth profile was split into four unequal sections, where each section line represents a change in composition as a function of depth.
2) For each section the atomic percentage is integrated as a function of depth to obtain the relative number of each of the Cu, In, and Se atoms.
3) Calculate the proportion of phases present in each section based on stoichiometric considerations assuming $CuInSe_2$ forms to the maximum of its ability followed by $Cu_2Se$ and $In_2Se_3$. Finally any remaining elements are assumed to be elemental. See table SIT1 for a summary of the phases present in the four sections of the film.
4) Sum the quantity of each phase from all the sections to form a total amount of each phase present in the sample.
5) Estimate Gibbs free energy by assuming it is a molar fraction weighted simple addition of contributions of Cu reacting to form $Cu_2Se$, and then the reaction of the binary selenides to form the ternary.

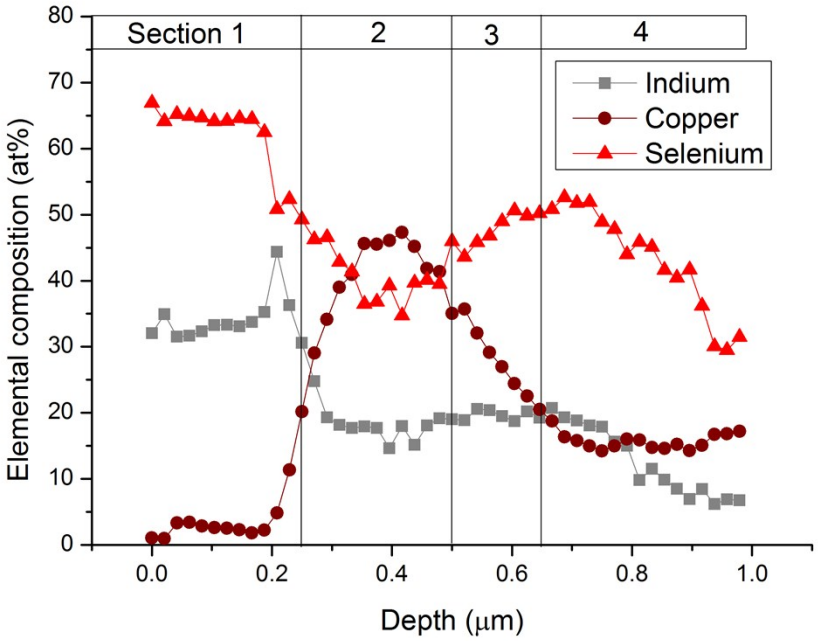


Figure SI1 Depth profile of a as coelectrodeposited sample. Data re-plotted from reference [1].

| Compound / Element | Relative number of molecules of phase | | | | Mol fraction in total film |
|---|---|---|---|---|---|
| | Section 1 | Section 2 | Section 3 | Section 4 | |
| $CuInSe_2$ | 2.2 | 4.1 | 2.9 | 4 | 0.43 |
| $In_2Se_3$ | 3.7 | 0 | 0 | 0 | 0.12 |
| $Cu_2Se$ | 0 | 1 | 0.45 | 0.6 | 0.07 |
| Cu | 0 | 3.5 | 0 | 0 | 0.11 |
| Se | 1.9 | 0 | 0.85 | 5.5 | 0.27 |

Table SIT1. Summary of the determined composition of each of the film sections 1-4 indicated in Figure SI1. Values give the fraction that the mass of each compound contributes to the total mass of each film section.

**Free energy calculation:**

0.11 mol fraction Cu reacts to form 0.05 mol fraction $Cu_2Se$ leading to a contribution of -5 $kJmol^{-1}$.

0.12 mol fraction $Cu_2Se$ reacts with 0.12 mol fraction $In_2Se_3$ leading to a contribution of -1 to -5 $kJmol^{-1}$.

Therefore the total Gibbs free energy change is estimated to be between -6 to -11 $kJmol^{-1}$.

**Experimental validation of the calculated time temperature profiles**

In order to experimentally validate the calculated temperature time profiles for the samples undergoing laser irradiation we carried out the following experiment. A small thermal mass thermocouple was stuck to the back surface of the glass substrate of Cu-In-Se deposited sample, and the temperature was measured during laser irradiation. Since the model calculates the temperature at all points through the depth of the sample we hypothesized that if the calculated temperature at the back surface is similar to the experimentally determined temperature, the model and material constants used must be reasonable since the heating is driven by absorption on the front precursor surface.

The experimental setup is shown in figure SI2(a). In order to study the robustness of the model we experimentally changed the glass thickness as well as the irradiation time. The experimental and calculated profiles are shown in figures SI2(b) and (c).

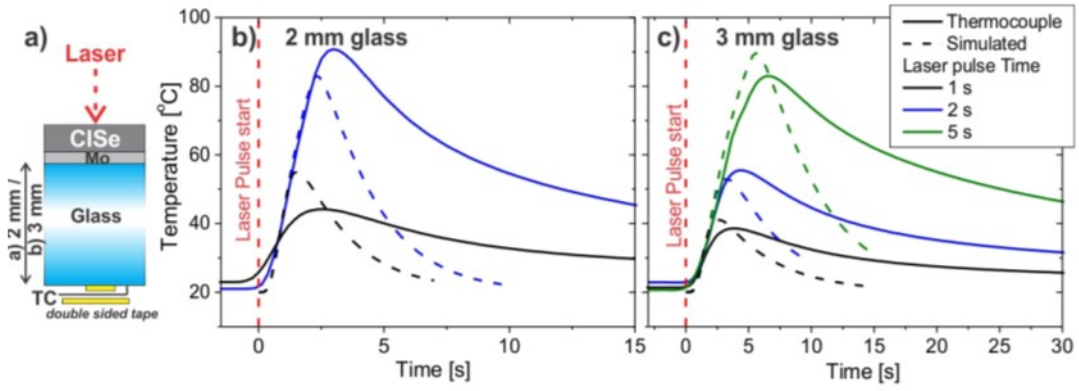


**Figure SI2(a) experimental setup and temperature time profiles at the back of the substrate measured (solid line) and calculated (dashed line) on (b) 2mm glass and (c) 3mm glass. Laser irradiation was fixed at 150 Wcm-2.**

For all laser irradiation times and glass thicknesses, the initial calculated heating ramp profiles agree well with the experimentally determined profiles. Similarly, the maximum peak temperatures are also in good agreement within 10°C of one another. Where the model diverges from the experimental results is in the cooling of the glass after the maximum temperature is reached. Experimentally the rear of the glass is found to cool slower than the model predicts. An explanation for this is the fact that in the model the adhesive pad of the thermocouple was not accounted for, since its properties are unknown, but it would act as a thermal insulator slowing the cooling and explain the discrepancy that we observe. Overall the calculated results fit the experimentally determined ones well suggesting the model is functioning correctly. Nonetheless, because steady state conditions are not met and the temperature gradient is not uniform through the depth of the sample and substrate, we could expect a 50 to 100°C error in the irradiated thin film surface temperature.

**Evidence of $Cu_{2-x}Se$ melting at the surface only**

The top view SEM images of the binary chalcogenide layer in Figure 3II of the main manuscript show the sharp platelet edges of the Cu-Se phase blurring upon 1064 nm laser irradiation. To better illustrate the melting phenomena of the top of the plates due to surface irradiation, here in figure SI2 we compare cross sectional images before and after laser annealing.

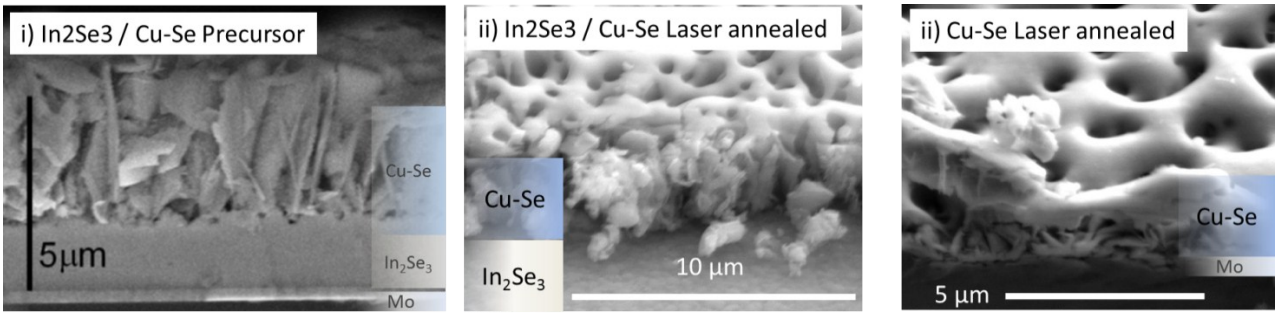


Figure SI3 Binary chalcogenide layer (i) precursor and (ii) after laser annealing using 1064 nm excitation.(iii) Cu-Se only on molybdenum. Note laser annealing in (ii) & (iii) was carried out with 5 shots of 125 mJ/cm$^2$ laser pulses. In this case pulse annealing and continuous wave annealing lead to similar results.

Figure SI3i) is an image of the precursor similar to figure 1bii) of the manuscript. After laser annealing with sufficient energy the Cu-Se surface begins to melt as shown on the surface of the film in figure SI3ii). Debris obscures clearly observing the platelet structure underneath. However figure SI3iii) shows an image of a similarly laser annealed Cu-Se layer deposited on Mo with a melted top surface and the buckling plates underneath.

**Simulation of spatially and time dependent distribution of temperature during 1 second laser annealing of a Cu/In/Se.**

A short video of the three dimensional temperature simulation is included in the supplementary information. It shows how the temperature evolves as a function of time, and how the temperature distributes itself laterally. In the manuscript the peak temperature at any moment in time is plotted.

**Maximum temperature heat profile during rastering of laser beam**

In order to determine the peak temperature of the CISe film during annealing, a finite element model was constructed, where the spatial and time dependent temperature of the sample is calculated during a typical process where the laser rasters over the film. To construct this model, finite element modelling using the COMSOL software is employed. The beam is assumed to be a perfect Gaussian with its spread and peak power calculated from the differential in beam flux before and after the 2 mm aperture. The power dissipation within the sample stack is calculated using a transfer matrix code from the refractive index, *n* and extinction coefficient, κ, values of $CuInSe_2$ and Mo ($CuInSe_2$: $n = 3.1$, $\kappa = 0.15$, Mo: $n = 2.4$, $\kappa = 4.4$). Heat transfer within the film is via conduction and radiative and convectional cooling is assumed from the CISe/air interface. Figure SI4 shows a contour plot of the spatial dependence of the maximum temperature for two passes of the laser beam over the sample. The simulated peak temperature varies from around 400 °C (673 K) in the coldest part of the film to 750°C (1023 K) at the hottest part of the film near the edges of the glass as the laser beam exits.

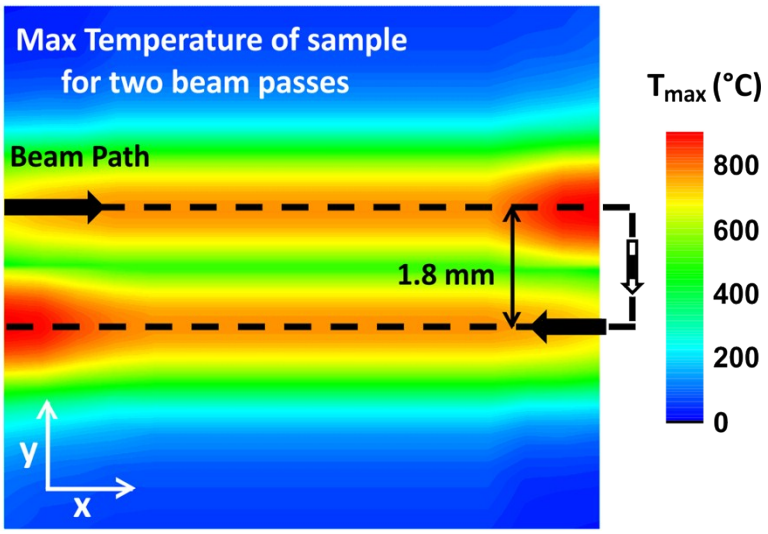


Figure SI4 Maximum surface temperature map of $CuInSe_2$ film for two passes of the rastered 150 W/cm$^2$ laser beam.

It is interesting to compare the photographs of a Cu-In-Se co-deposited precursor before and after laser annealing. Before annealing the precursor displays no obvious patterns (figure SI5(a)). The metallic molybdenum border is not covered in Cu-In-Se as it is taped off with isolating kapton tape during the electrodeposition. After rastering the laser, the appearance of the sample consists of stripes in the direction that the laser passed (figure SI5(b)). Note how near the edges of the semiconductor material that the stripe flares out, similar to how the heat flow model predicts. The molybdenum edge is now oxidized on the surface due to reaction with selenium vapour, and hence it has changed colour.

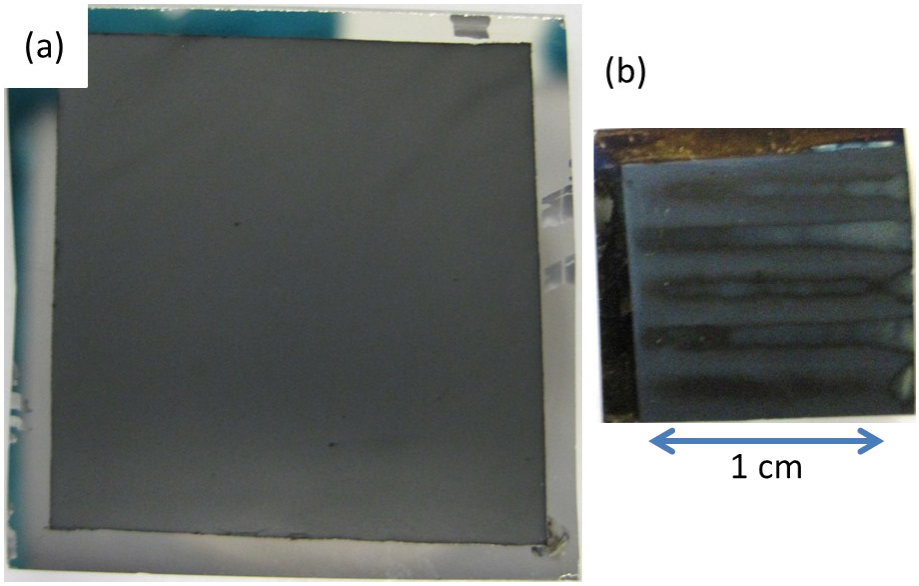


Figure SI5(a) Typical co-electrodeposited Cu-In-Se precursor sample and (b) CISe sample after laser annealing with a 2 mm wide, 150 $W.cm^{-2}$ beam rastered over the surface. 2.5 x 2.5 $cm^2$ precursors are cut into four, and here a single quarter has been laser annealed.